Chemotactic behavior of spermatozoa captured using a microfluidic chip

Shweta Bhagwat,[1] Shraddha Sontakke,[1,2] Deekshith K.,[1] Priyanka Parte,[2,a)] and Sameer Jadhav[1,a)]
[1]*Department of Chemical Engineering, Indian Institute of Technology Bombay, Powai, Mumbai 400076, India*
[2]*Department of Gamete Immunobiology, Indian Council of Medical Research-National Institute for Research in Reproductive Health, Parel, Mumbai 400012, India*

(Received 25 January 2018; accepted 20 March 2018; published online 29 March 2018)

Chemotaxis, as a mechanism for sperm guidance *in vivo*, is an enigma which has been difficult to demonstrate. To address this issue, various devices have been designed to study sperm chemotaxis *in vitro*. Limitations of traditional chemotaxis devices were related to the inability to maintain a stable concentration gradient as well as track single sperm over long times. Microfluidics technology, which provides superior control over fluid flow, has been recently used to generate stable concentration gradients for investigating the chemotactic behavior of several cell types including spermatozoa. However, the chemotactic behavior of sperm has not been unequivocally demonstrated even in these studies due to the inability to distinguish it from rheotaxis, thermotaxis, and chemokinesis. For instance, the presence of fluid flow in the microchannels not only destabilizes the concentration gradient but also elicits a rheotactic response from sperm. In this work, we have designed a microfluidic device which can be used to establish both, a uniform concentration and a uniform concentration gradient in a stationary fluid. By facilitating measurement of sperm response in ascending, descending ,and uniform chemoattractant concentration, the assay could isolate sperm chemotactic response from rheotaxis and chemokinesis. The device was validated using acetylcholine, a known chemoattractant and further tested with rat oviductal fluid from the estrus phase. *Published by AIP Publishing*. https://doi.org/10.1063/1.5023574

I. INTRODUCTION

The journey of a sperm into the female genital tract involves certain mechanisms that direct the sperm towards the oocyte for fertilization.[1–4] These guidance mechanisms are under active investigation to better understand the cues governing the homing of the sperm to the site of fertilization. These cues could be related to fluid flow—demonstrating rheotaxis,[5–7] mediated by the temperature gradient—indicating thermotaxis,[8,9] and in response to the chemical gradient—suggestive of chemotaxis.[10] Although most sperm demonstrate rheotaxis,[5–7,11] only a small fraction exhibit thermotaxis[12] and chemotaxis,[13–18] as the latter two are known to occur once the sperm undergoes capacitation. It has been demonstrated that approximately 2%–12% of the total population are chemotactically responsive at a given instance.[14,16,19] Interestingly, one study employing a Zigmond chamber showed 20%–35% increase in the directionality towards allurin and follicular fluid.[18]

Sperm across most species are known to exhibit a chemotactic response to various chemoattractants identified from their natural milieu.[2] Human follicular fluid[20] was the first to be identified as a chemoattractant. Later, Oliveira and co-workers investigated chemotactic response of mouse sperm to oviductal and follicular fluid.[17] Several groups have examined sperm

[a)]Authors to whom correspondence should be addressed: partep@nirrh.res.in and srjadhav@iitb.ac.in

chemotactic response to individual components of these fluids for identification of the most probable chemoattractants. Some of the confirmed chemoattractants are the atrial natriuretic peptide,[21] progesterone,[15,22,23] allurin,[18] Natriuretic Peptide type C (NPPC),[24] Chemokine Receptor 6 (CCR6),[25] and Regulated upon Activation, Normally T-Expressed, and presumably Secreted (RANTES),[26] while others considered to be putative chemoattractants include acetylcholine (ACh). There are contradictory results obtained with progesterone, where some have reported that progesterone induces only chemoattraction with no change in motility,[27] whereas few have demonstrated that progesterone is a weak chemoattractant.[28] Although progesterone is the main steroid present during ovulation surrounding the egg microenvironment,[29,30] there may be other contenders that could be more potent as chemoattractants as compared to progesterone. ACh is known to have its origin from follicular fluid[31] found in the oviduct. Detection of ACh and localization studies of the ACh synthesizing enzyme have also been reported in porcine oviductal epithelium.[32] ACh has also been shown to participate in regulating ovarian functions *in vivo* in the rat.[33] This study demonstrated that inhibiting acetylcholinesterase *in vivo* increased intra-ovarian acetylcholine which in turn enhanced the follicular development and fertility in the female rats. Thus, as acetylcholine is secreted in the oviduct during ovulation and acetylcholine receptors are present on sperm, it may have a role in inducing chemotaxis. Previous work also shows increased migration of the mouse spermatozoa, towards 1 mg/ml ACh source.[31]

The development of microfluidics technology has facilitated generation of stable concentration gradients in fluid systems.[34] Recently, mouse sperm chemotaxis to ACh was shown in a microfluidic device[35] where progressive sperm were separated from non-progressive ones. Microfluidic devices have also been used in efforts to distinguish chemokinesis from chemotaxis of sperm.[36–38] In one of these studies, sperm diffusivity towards a chemoattractant reservoir was measured as an estimate of chemokinesis in a microfluidic channel.[38] However, the concentration distribution of the chemoattractant was not characterized in the aforementioned study. In other studies, chemokinesis was estimated from the change in the average curvilinear velocity of the sperm in response to the presence of a chemical gradient while the biased sperm motion in the direction of increasing chemoattractant was used as a measure of chemotaxis.[36,37] However, the absence of a time-invariant concentration distribution or the presence of fluid flow in these studies could possibly have led to chemokinetic and rheotactic response influencing sperm chemotaxis. Therefore, to facilitate a better understanding of mechanisms governing sperm guidance to the egg, there is a need to develop new methods for controlling the sperm microenvironment and analyzing sperm motility.[39]

An accurate quantitation of chemokinesis and chemotaxis requires the absence of fluid flow and convective transport in the test region such that constant and uniform properties (concentration or concentration gradient) are maintained while measuring sperm motion. Recently, we have used computational fluid dynamics to design and optimize a novel microfluidic device to generate robust uniform concentration gradients that are able to withstand flow fluctuations.[40] In the present work, we have modified and experimentally validated the design for its ability to generate uniform chemical gradients, as well as adapted it to study sperm chemotaxis and chemokinesis. The microfluidic device, which has two inlets and two outlet streams, facilitates not only the concentration profile in the test region to remain time-invariant, but also suppresses hydrodynamic flow in the test region. Using rat sperm, we tested the ability of the device to demonstrate chemotaxis, first with a single chemoattractant—ACh, and later with Oviductal Fluid (OF), which is known to contain a pool of chemoattractants. Additionally, to distinguish chemotaxis from chemokinesis, we tested sperm response to a uniform concentration of the aforementioned chemoattractants.[2,26] Fertilization success has been reported for sea urchin sperm that were chemotactic, where they found that removing the sperm chemoattractant decreased the fertilization ability.[41] Hence, chemotaxis can also be considered as a selection method for improving the fertilization rate and embryo quality during *in vitro* culture. The study outcome has a direct impact on the use of chemotaxis to selectively isolate good quality sperm for IVF (*In Vitro* Fertilization).[42] The device can also be used to identify putative chemoattractants and test different biological fluids for the presence of chemoattractants.

II. MATERIALS AND METHODS

All experiments were performed in compliance with the guidelines and approval of the Institutional Animal Ethics Committee of Indian Council for Medical Research-National Institute for Research in Reproductive Health (ICMR-NIRRH), Mumbai.

A. Modelling and simulation of the microfluidic device

Modelling and simulation of the microfluidic device was carried out using the COMSOL multi-physics® software, version 5.2 (COMSOL® Inc., Burlington, MA). As shown in Fig. 1, the device comprised of two inlets, I_1 and I_2, carrying the aqueous chemoattractant solution and water, respectively. The inlets met at the contact zone to equilibrate any pressure or flow rate differences between the two streams prior to their separation into long channels that connect to relatively wide main channels.[43] The main channels are connected by several narrow transverse channels, after which they unite to form the primary outlet O_1. A secondary outlet O_2 removes the fraction of streams. The long channels from the contact zone are required to allow complete mixing of fluid from the contact zone that results from diffusive and convective mixing of the two inlets and ensure that the fluid entering the main channels contains a uniform chemoattractant.[43] Two connecting channels to the main channels emanate from the cell reservoir, through which sperm swim into the test zone. The depth of each of the channels in the device is 55 μm, while the planar dimensions of each element in the device and the test zone are as shown in Fig. 1. Physiologically, the cross-sectional dimensions of the ampulla and the isthmus typically have a range of 10–80 μm.[44] To mimic these *in vivo* conditions, we have chosen the dimensions of the microfluidic channel as 55 μm × 55 μm.

Finite element simulations were carried out in COMSOL by solving the mass and momentum conservation equations for an incompressible Newtonian fluid (water with density and

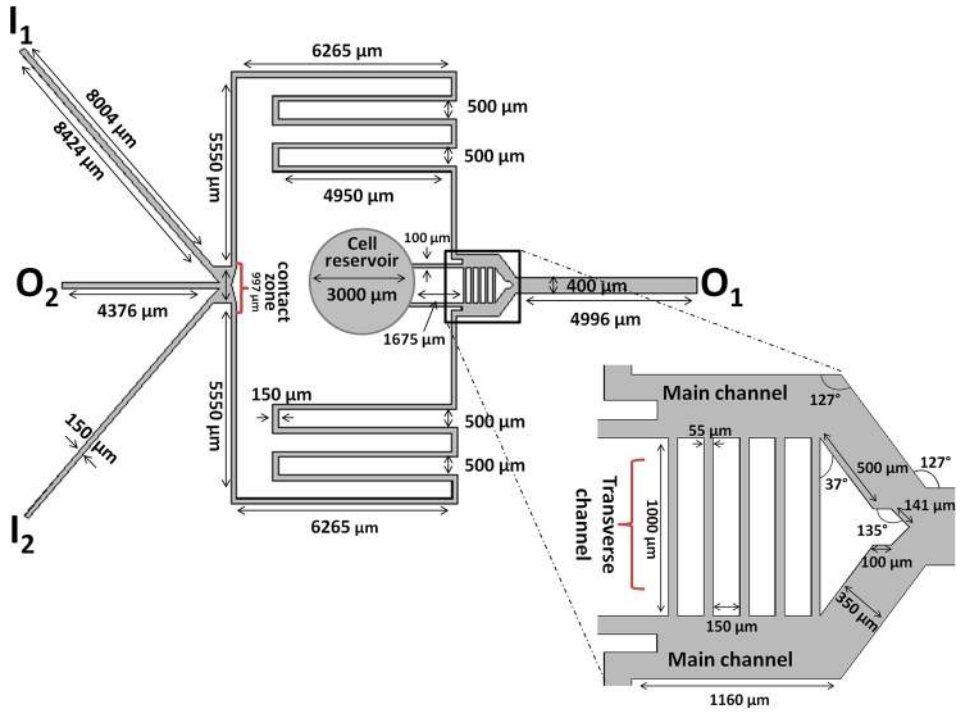

FIG. 1. Microfluidic device design and dimensions. A model of the basic device geometry drawn in COMSOL Multiphysics 5.2, which consists mainly of two inlets, chemoattractant input (I_1), and diluent input (I_2); two outlets, Outlet$_1$ (O_1) and Outlet$_2$ (O_2); a small contact area termed as the "contact zone"; and the cell reservoir from which the sperm enter the main channels. The dimensions of the device are mentioned for each section in μm. A close-up view of the test zone (magnified as an inset) consisting of two main channels that join to form the transverse channels. The angular measurements of the corners are specified in degrees and dimensions of the channels are listed in μm.

viscosity 1000 kg/m^3 and 1 cP, respectively) and a species conservation equation for the solute (chemoattractant with diffusivity 3.5×10^{-10} m^2/s). A fluid velocity of 2×10^{-3} m/s was used for each inlet stream and a pressure of 0 Pa was used for the outlets. No-slip and impervious surface boundary conditions were used for all other surfaces. The steady-state simulation results were analyzed for estimating the concentration profile in the transverse channels.

B. Fabrication of the microfluidic device

The design of the microfluidic device, with dimensions as mentioned in Sec. II A and detailed in Fig. 1, was printed on a photomask transparency sheet.[45] The silicon master was fabricated using the soft lithography[46] technique in a clean room facility. First, a negative photoresist (Su-8 2050; Microchem Corp., Westborough, MA, USA) was spin-coated on a cleaned 2-in. silicon substrate having a 500 nm silicon dioxide surface layer (500 rpm/10 s followed by 3000 rpm/30 s). The wafer was then prebaked on a hot plate at 65 °C for 3 min and later at 95 °C for 9 min. Photolithography was then carried out on the wafer using a MJB4 mask aligner (Karl Suss, Garching, Germany) with exposure to UV light (350 nm) with an energy of 180 mJ/cm^2. The wafer was then subjected to post-exposure baking for 2 min at 65 °C and 7 min at 95 °C. The micro-pattern was developed by dipping the wafer in the Su-8 developer for 5 min (Microchem Corp., Westborough, MA, USA). The silicon master was then washed with 2-propanol, air dried, and hard baked for improved adhesion of the photoresist to the silicon wafer. The depth of the SU-8 master, measured with a stylus profiler (Dektak 150, Veeco Instruments, Inc.), was estimated to be 53.19 ± 7.06 μm.

The micropattern from the silicon master was transferred on to a polydimethyl siloxane (PDMS) slab using the silicone elastomer kit (Sylgard® 184, Dow Corning Corp., Midland, MI, USA). To this end, a mixture of PDMS and a curing agent at a ratio of 10:1 was poured on the silicon master and allowed to polymerize overnight at 50 °C in a hot air oven. The PDMS slab was cut to size and 1.5 mm diameter holes were punched over the inlets and outlets while the cell reservoir had a diameter of 3 mm. The PDMS slab was then bonded to a glass slide (76 mm × 26 mm) using oxygen plasma generated in a plasma cleaner[47] (PDC-32G-2, Harrick Plasma, Ithaca, NY, USA).

C. Isolation of oviductal fluid

Three-month-old Holtzman inbred female rats were sacrificed by CO_2 asphyxiation in their ovulatory (estrus) phases. The oviductal fluid was collected by flushing the oviduct with 0.25 ml of Dulbecco's minimum essential medium (DMEM) through a 1 ml tuberculin syringe connected to a needle (30 gauge). Only fluid samples that contained fertilizable oocytes were considered for the study. However, care was taken to exclude the oocytes from the collected fluid samples. The fluid thus collected was centrifuged at 2000 g (4600 rpm) for 5 min at 4 °C to get rid of any cellular debris. The protein content in the supernatant of the collected oviductal fluid was quantified using Bradford's method.[48] The supernatant samples were snap frozen and stored at −80 °C until further use.

D. Preparation of spermatozoa

Sexually mature three-month-old Holtzman inbred male rats were sacrificed by CO_2 asphyxiation. The scrotal region was cleaned and dissected to obtain intact epididymides and care was taken to remove excess fat and blood vessels. The epididymides were immediately washed in saline and incubated in 5 ml DMEM (Thermo Fischer Scientific, Waltham, Massachusetts, USA) pre-equilibrated with 5% CO_2. The cauda epididymides were excised from the intact tissue and one longitudinal cut was made to allow the sperm to swim up in 5 ml of DMEM, pre-equilibrated with 5% CO_2 in 50 ml centrifuge tubes. The media containing the swim-up sperm was collected in a tube and the sperm concentration was maintained to 2×10^6 cells/ml. 4.5 ml of this sperm suspension was then subjected to capacitation with 2%

Bovine Serum Albumin (BSA).[49] The sample was incubated in 5% CO_2 at 37 °C for 2.5 h. 1.6×10^5 capacitated cells were used for each experiment.

E. Sperm motility assay

Sperm motility was manually quantified using a chamber prepared in-house by wrapping four layers of scotch tape 3 cm apart on a 76 mm × 26 mm glass slide to give a chamber height of ∼200 microns. The sperm sample was diluted 1:10 (v/v) with DMEM containing two percent BSA and, 20 μl of this cell suspension was immediately loaded on the sperm motility chamber. A 22 × 40 mm coverslip was used to cover the chamber which was then mounted on an optical microscope (TE2000-U; Nikon Instruments Inc., Melville, NY, USA) equipped with a heated chamber (maintained at 37 °C) and a sCMOS camera (Orca Flash 2.8, Hamamatsu Photonics Inc., Japan). Images of the sperm sample were recorded at 45 fps for 10 s and the percentage of motile sperm was identified[50] from a sample count of greater than 100 cells. Sperm motility was estimated immediately after preparation of the spermatozoa sample, after 2.5 h and at the end of the experiment (<5.5 h). Only those chemotaxis assays where sperm motility remained >70%[51] till the end of the experiment, were included in the study.

F. Microfluidic perfusion set-up for chemotaxis assays

The microfluidic device was first perfused with 1% (w/v) BSA in distilled water to prevent sperm adherence to the walls of the device. The device was then flushed with DMEM media to remove excess BSA. A 250 μl capacity polypropylene microcentrifuge tube was cut at the bottom and inserted in the 3 mm cell reservoir hole of the PDMS device and filled up to the brim with DMEM to avoid the presence of air bubbles. The fluid connections from the device inlets comprised of 1 mm (inner diameter) silicone tubing, which were connected to a 1 ml tuberculin syringe (BD, Franklin Lakes, NJ, USA). The silicone tubes from the primary and secondary outlets were joined to a T-connector, the outlet of which was connected to a 1 ml syringe mounted on a syringe pump (NE-1000, New Era Pump Systems Inc., Farmingdale, NY, USA) (Fig. 2).

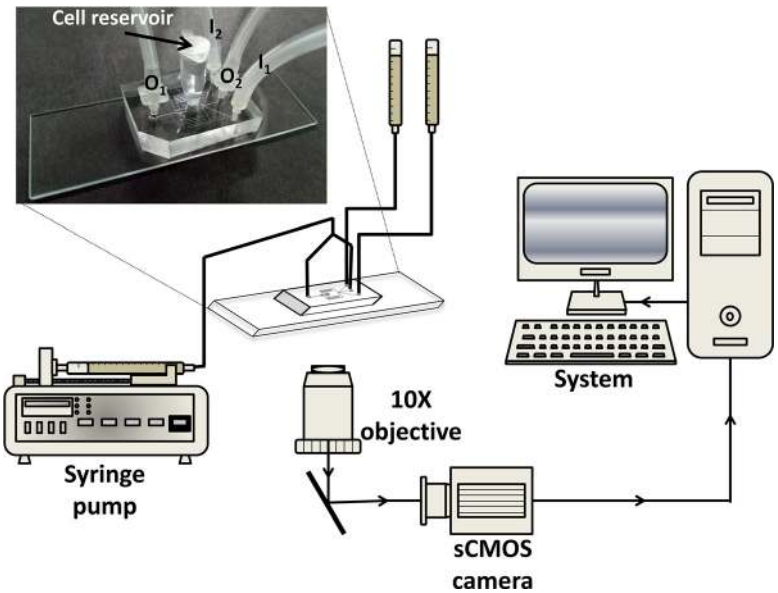

FIG. 2. Experimental set-up for the chemotaxis assay. Schematic representation of the experimental set up with an inset image of the PDMS device bonded on a glass slide with tubing connections to inlets (I_1 and I_2) and outlets (O_1 and O_2); and a port in the center for the sperm reservoir. This microfluidic device set-up is positioned on a microscope stage and the fluidic connections for the inlets and outlets are made as shown, with flow controlled using a syringe pump. The video frames of sperm moving in transverse channels are recorded using a sCMOS camera and stored on a computer hard drive.

G. Generation of a uniform concentration gradient in the microfluidic device

To ensure that a uniform concentration gradient is formed in the transverse channels of the microfluidic device, the chemoattractant and diluent inlets were filled with an aqueous solution of 0.5 mM fluorophore propidium iodide (absorbance at 493 nm, emission at 636 nm; Sigma-Aldrich Corp., USA) and water. The microfluidic device was mounted on the stage of a laser scanning confocal microscope (LSCM; LSM780, Carl Zeiss Microscope, Thornwood, NY, USA). A syringe pump was used to aspirate the fluid at a rate of 1 μl/min from the tube connecting the two outlets to the pump such that the flow rate of 0.5 μl/min was achieved in each inlet. Polystyrene beads having a mean diameter of 5 μm, were introduced into each inlet stream at a concentration of 15 000 particles/ml (Sigma-Aldrich Corp., USA). The polystyrene microbeads in the transverse channels remained stationery confirming that fluid flow and convective transport of the solute do not occur in these channels. This ensured that a uniform concentration gradient resulted from purely diffusive transport across the transverse microchannels. LSCM Confocal images of the transverse channels were acquired using a plan apochromat objective (magnification: 10×, NA: 0.45) through a band pass filter 562–695 nm. The concentration profile obtained after gradient generation in the transverse channels was then quantified by measuring the fluorescence intensity using the ImageJ software[52] (ver.1.50b, NIH, USA) along the length of each transverse channel (averaging 9 frames) for each channel.

H. Chemotaxis assay

For the chemotaxis assays, the syringe connected to the chemoattractant inlet I_1 of the microfluidic device was filled with either 2.76 mM or 5.51 mM ACh solution (made from 100 mg/ml stock solution) in DMEM. The diluent inlet I_2 was filled with DMEM. The primed microfluidic device was mounted on the stage of an inverted microscope which was enclosed in a chamber maintained at 37 °C. The two syringes connected to the inlet were also mounted in this enclosure such their fluid levels were identical (Fig. 2). As described in the previous Sec. II G, a uniform concentration gradient was allowed to develop in the transverse channel by aspirating fluid at a rate of 1 μl/min from the tube connecting the two outlets from the microfluidic device to the pump such that the flow rate of 0.5 μl/min was achieved in each inlet. Uniform concentration gradients were generated having a magnitude of 2.76 M/m and 5.51 M/m, corresponding to 2.76 mM and 5.51 mM ACh solutions, respectively. After flow stabilization and gradient formation, 80 μl of sperm sample at a concentration of 1.6×10^5 cells/ml was added to the cell reservoir. The flow and gradient were allowed to stabilize for 10 min, after which sperm motion in the transverse channels was recorded at 10× magnification using the sCMOS camera to capture 1920 × 720 pixel^2, 8-bit grey scale images at 88 fps for 15 s. Each experimental run was carried out for 1 h to record ∼40 such movies of 15 s duration and a maximum of 3 runs were carried out for each sample.

To study chemokinesis, syringes connected to both inlets were filled with DMEM with either 2.76 mM or 5.51 mM ACh solution in DMEM. As a negative control, syringes connected to both inlets were filled with DMEM (without ACh). To study the chemotactic response of sperm to oviductal fluid, experimental runs were conducted similar to those using ACh. To this end, three experimental runs were conducted with each pooled oviductal fluid sample containing ∼0.38 g/l protein content, which comprised of (i) chemotaxis assay (G) with oviductal fluid in inlet I_1 and DMEM in inlet I_2, (ii) chemokinesis assay (N) with oviductal fluid in both inlets I_1 and I_2, (iii) control assay (M) with DMEM in both inlets I_1 and I_2.

I. Estimation of number and velocity of sperm entering the transverse channels

We next investigated the chemotactic response of sperm to ACh or oviductal fluid. The straight line velocity (VSL) of the sperm moving from left to right in the transverse channels and those moving from right to left was estimated. For this purpose, only those sperm that could be tracked for at least 100 frames (1.14 s) were included in the count. The VSL was calculated by dividing the distance between initial and final positions of the sperm heads by the

time elapsed. A percentage frequency distribution of velocity was constructed for sperm moving in (i) ascending and (ii) descending concentrations of ACh/oviductal fluid, and(iii) uniform concentration of ACh/oviductal fluid and (iv) media devoid of ACh/oviductal fluid. The mean VSL for each of the aforementioned cases was calculated. The percent of sperm with velocities greater than 85 μm/s was also calculated for each case. Of the total sperm entering the transverse channels, the fraction entering from the left end of the transverse channels was obtained from all the recorded images. The test for asymmetry or biasedness of sperm entering the transverse channels was considered positive when this fraction differed significantly from 0.5.

J. Design of experiments and statistical analysis of data

Twenty male rats were used to obtain sperm samples for experiments related to chemotactic and chemokinetic responses to acetylcholine along with the DMEM control ($n \geq 4$). To account for variability in the time of exposure to each experimental condition, the sperm were exposed to two of the three experimental conditions for each experimental run and the sequence of exposure was shuffled (GM, MG, GN, NG, MN, and NM). The population size for each sample measurement was $n \geq 365$.

For the experiments with oviductal fluid, six independent samples were used with the protein concentration maintained at ~0.38 g/l for each experiment. Each oviductal fluid sample comprised of fluid from a single female rat or as a pool from up to 4 female rats. Fourteen female rats in their estrus phase were sacrificed. Six independent sperm samples were collected from six male rats for the experiments. The sequence of experimental runs ($n = 6$) was GMN, MNG, NGM, GNM, MGN, and NMG.

All data sets (for M, G, and N) were analyzed using the Prism 6 software (GraphPad Software, Inc., La Jolla, CA, USA). The estimation of asymmetry in sperm entering the two ends of the transverse microchannels was analyzed using the one sample t-test. Normality test for velocity distribution of sperm populations was carried out using the Shapiro-Wilk test. Since the VSL values showed a non-normal distribution, a non-parametric ANOVA (Kruskal-Wallis test) was used with Dunn's post-test for multiple comparisons. The differences were considered statistically significant when $p \leq 0.05$.

III. RESULTS AND DISCUSSION

A. Generation of uniform concentration gradient in the microfluidic device

To ascertain that the proposed design of the microfluidic device supported a stable and uniform concentration gradient of the chemoattractant, we first carried out the numerical simulation of fluid flow and transport of the chemoattractant in the device. The distribution of the chemoattractant in the microfluidic device as predicted by the simulation is shown in Fig. 3(A), while the test zone of the device is magnified to show the concentration distribution of the chemoattractant in the transverse channels [Fig. 3(B)]. A linear concentration profile of the chemoattractant was predicted by numerical simulation [Fig. 3(C)]. To validate the predictions of the numerical simulation, the microfluidic device was then fabricated and tested for the generation of a uniform concentration gradient of the fluorophore, propidium iodide. Confocal imaging [Fig. 3(D)] showed a gradient in fluorophore emission intensity along the length of the transverse channels thereby indicating the presence of a linear fluorophore concentration profile [Fig. 3(E)].

The linearity of fluorophore concentration as a function of axial position along the transverse channels had an R^2 value of ~0.98 and was found to remain time-invariant over the duration of the experimental run [Fig. 3(E)]. The uniform concentration gradient indicated that only diffusive transport was dominant in the transverse channels. When polystyrene beads of 5 μm diameter were introduced under steady flow conditions in the device, their position in the transverse channels remained unaltered over time, thereby confirming that convective transport in the transverse channels was negligible (data not shown). In accordance with previous studies,[36,45] the concentration gradient continued to remain stable and uniform as long as the syringe

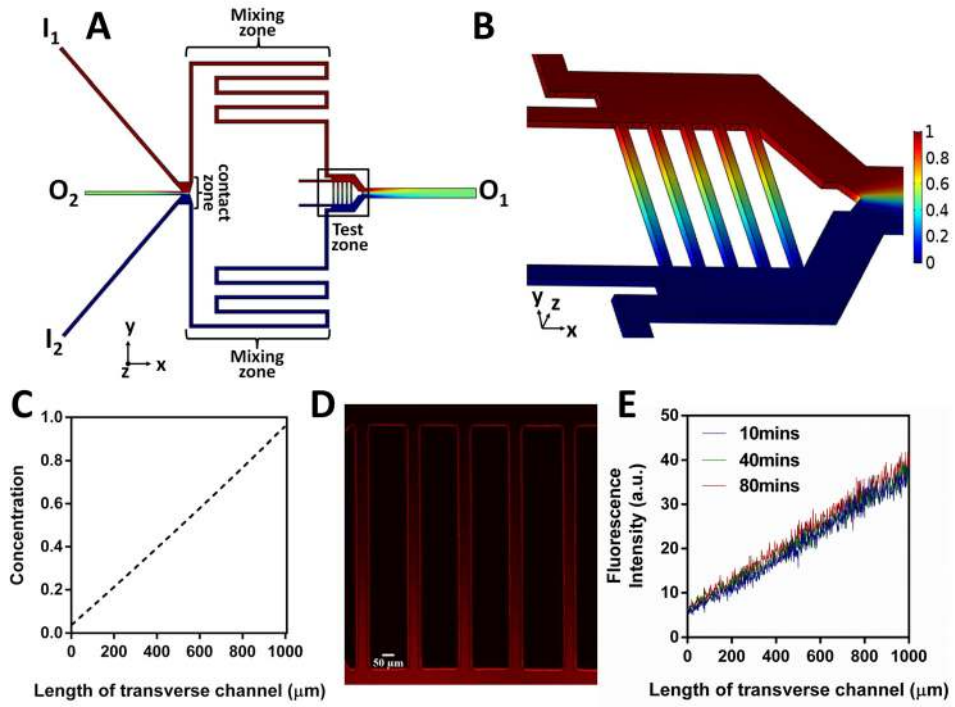

FIG. 3. Uniform concentration gradient in the microfluidic device. Simulation results in 3-D for gradient formed in the microfluidic device; concentration in I_2 (Blue) = 0 mol/m^3, I_1 (Red) = 1 mol/m^3; Velocities at both inlets: 1×10^{-3} m/s Pressure at outlet: 0 Pa, transverse channel width: 55 μm and length: 1000 μm. Concentration profile (Non-dimensionalized with the maximum concentration) obtained after COMSOL simulation in the entire device (A). A mixing zone between the contact area and the test zone allowed mixing of the inlet streams. Enlarged 3-D view of the transverse channels (Test zone); the scale bar on the right represents the concentration range of the gradient (B). Concentration gradient profile in the transverse channels after COMSOL simulation (C). LSCM imaging of gradient generated in the transverse channels of the device using 0.5 mM propidium iodide (D). Experimental results obtained using 0.5 mM propidium iodide shows a linear and stable gradient over time (E).

pump maintained a steady flow in the main channels of the microfluidic device [Fig. 3(E)]. In contrast, in a study related to gradient generation with gravity-driven flow for a longitudinal or horizontal gradient profile, the uniformity of the concentration gradient varies with time.[35]

B. Effect of ACh concentration gradient on sperm entry into the transverse channels

Sperm were allowed to swim into the test zone (Fig. 1) in a symmetric manner, with the expectation that the concentration of cells near the two ends of the transverse channels did not differ significantly. To examine whether the presence of ACh concentration gradient affected sperm entry into the transverse channels, we measured the number of sperm entering the transverse channels in increasing (left to right) and decreasing (right to left) concentration of ACh [Fig. 4(A)]. In the absence of a chemotactic response, it is expected that the fraction of total sperm entering the transverse channels from either end should be symmetric and equal to 0.5. However, in the presence of a gradient concentration of 2.76 M/m and 5.51 M/m ACh, the fraction of sperm entering the transverse channels from the left end was 0.6 and differed significantly from the expected value [Fig. 4(B)]. This suggested that ~20% more sperm entered the transverse channels in the direction of increasing ACh concentration in comparison to sperm entering in the vice-versa direction. As expected, in the presence of uniform ACh concentrations of 2.76 mM and 5.51 mM, as well as in the absence of the chemoattractant, the fraction of sperm that entered the transverse channels from the left end was not significantly different from 0.5, suggesting that an equal fraction of sperm entered the transverse channels from each end [Fig. 4(B)].

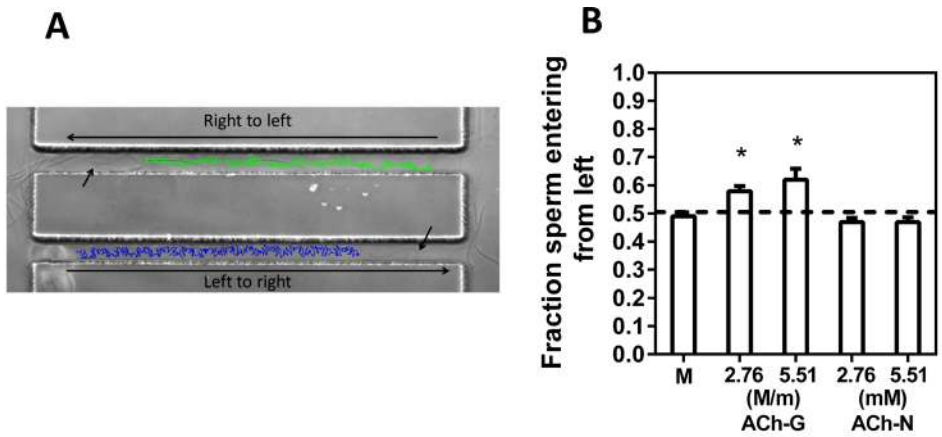

FIG. 4. The directionality of sperm in the transverse channels in the presence of media or chemoattractant. Sperm tracks with schematic illustration of sperm (denoted by an arrow) swimming from left to right (blue track, increasing concentration) and right to left (green track, decreasing concentration) in the transverse channels (A). The fraction of sperm entering the transverse channels from the left end in a linear gradient of ACH (ACh-G), uniform concentration of ACh (ACh-N) and media (M) was determined (B). The assay was performed using 2.76 mM and 5.51 mM of ACh in DMEM. The results are cumulative for 20 experiments in total with different combinations as described in Sec. II. Each column represents mean values (±SEM) for the individual conditions. Sperm traveling in a gradient of ACh concentration (2.76 M/m and 5.51 M/m) are preferentially directed along increasing ACh concentration as compared to those in other conditions. Statistical significance was determined by one sample t-test. "*": $p < 0.05$.

It has been reported that relatively larger number of mouse sperm migrate into microchannels that contained an ACh gradient thereby showing that ACh is a chemoattractant for mouse sperm.[31,35] Given that mammalian sperm chemotaxis lack species specificity,[53] the increase in the fraction of sperm moving along an increasing ACh concentration gradient, suggest that rat sperm also respond chemotactically to ACh.

C. Effect of ACh concentration gradient on straight line velocity of sperm

For both chemotaxis and chemokinesis, it is the speed of the sperm that increases. However, the directional increase in straight line velocity (VSL) in the presence of a concentration gradient vis a vis uniform concentration of chemoattractant differentiates the two. To discern this, we estimated the effect of the ACh gradient and uniform ACh concentration on the mean VSL of sperm population entering the transverse channels. The mean VSL was observed to be significantly higher in the case of sperm population moving along increasing ACh concentration in comparison to that moving along a decreasing concentration of the chemoattractant [Fig. 5(A)]. This was observed with both 2.76 M/m and 5.51 M/m of ACh [Fig. 5(A)]. The mean VSL for sperm moving along the decreasing gradient or a uniform concentration of 2.76 mM ACh was similar to that for sperm swimming in media alone [Fig. 5(A)]. Interestingly, at a uniform concentration of 5.51 mM, the mean VSL was significantly lower compared to that of ACh at 2.76 mM and media alone [Fig. 5(A)]. As sperm response to ACh is rapid, we speculate that ACh receptors on sperm may be nicotinic.[54,55] At higher concentrations of ACh, its cognate receptors on sperm may get refractory, such that sperm no longer respond to ACh and this is reflected as a decrease in the mean VSL of sperm at 5.51 mM. This is also evident from the frequency distribution of the same [Fig. 5(C)]. However, this reduction is not seen when sperm are exposed to gradient concentrations of 5.51 M/m.

Sperm demonstrated an array of velocities when exposed to media, uniform or gradient concentration of ACh. We, therefore, sought to analyze the distribution pattern of VSL by plotting the percentage frequency distribution of the cumulative VSLs obtained for the three conditions with both 2.76 mM ACh [Fig. 5(B)] and 5.51 mM ACh [Fig. 5(C)]. The velocity distribution profile showed a shift in the curve for 2.76 M/m gradient L-R as compared to gradient R-L and the controls. With a 5.51 M/m gradient L-R curve, a plateau effect was observed, with

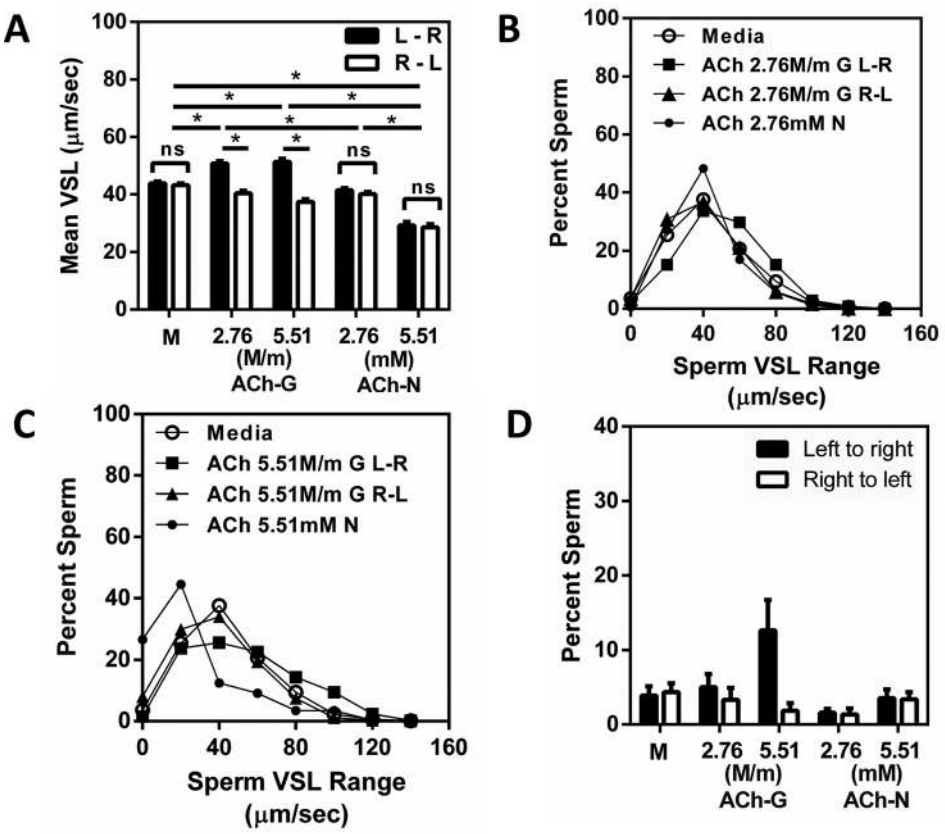

FIG. 5. Straight line velocities (VSLs) of sperm exposed to uniform or gradient concentrations of ACh. VSL was determined in the transverse channels for sperm exposed to either a gradient of ACh (ACh-G); a uniform concentration of ACh (ACh-N), at 2.76 and 5.51 mM ACh and the mean VSL was calculated for each group. Sperm exposed to media (M) devoid of ACh served as the control. The bar graph shows the mean VSL (±SEM) for sperm moving from Left to Right (L - R) and Right to Left (R - L) in response to the different conditions tested (A). Sperm VSLs are significantly higher when sperm move along the increasing concentration gradient of ACh compared to those moving along decreasing concentration (2.76 and 5.51 M/m) and the respective controls. The frequency distribution profile of velocity for sperm moving in media, increasing ACh Gradient (G L-R), decreasing ACh Gradient (G R-L), and uniform concentrations of ACh (N) 2.76 mM (B) and 5.51 mM (C). Sperm VSL distribution pattern showed a shift in the curve for 2.76 M/m gradient L-R and a plateau effect for 5.51 M/m gradient L-R, as compared to their respective controls with increased distribution towards higher VSL. A comparison of the percent sperm (±SEM) with VSL $\geq 85\ \mu$m/s in the different groups (D) showed a modest increase in the percentage of sperm exposed to a gradient of 5.51 M/m. The results are cumulative from 20 experiments in total with different combinations as described in Sec. II. "*": $p < 0.05$.

increased distribution towards higher VSL. From the curve, it is evident that in a L-R gradient of 5.51 M/m whilst most sperm moved at velocities ranging from 20 to 60 μm/s which is lower with respect to the percentage of sperm showing velocities in that range for the controls, very few but a significant number of sperm move at velocities $\geq$80 μm/s. We also observed that the velocity distribution for all the curves had a maxima at 40 μm/s [Figs. 5(B) and 5(C)] except for sperm exposed to a uniform concentration of 5.51 mM ACh, which had a maxima at 20 μm/s [Fig. 5(C)]. This explains the reduction in the mean VSL of sperm swimming in a uniform concentration of 5.51 mM ACh as compared to other conditions [Fig. 5(A)].

It has been reported that sperm VSL increases as they move along an increasing chemoattractant gradient.[36] Thus, we thought that it would be interesting to know the proportion of sperm moving with higher VSLs from the total population. To this end, we calculated the 95 percentile (that corresponds to 2σ) for the VSL distribution of sperm exposed to media alone, which gave us a value of 85 μm/s. This was used as a cut-off to categorize sperm population moving with a higher VSL, in all the conditions tested. We, therefore, divided the total sperm population into two groups that is sperm with VSLs in the range of 0–85 and $\geq$ 85 μm/s, and

calculated the percentage of sperm traveling with velocities $\geq$85 μm/s. We observed that there is a modest increase in the percentage of sperm showing VSL above 85 μm when exposed to an increasing ACh gradient at 5.51 M/m concentration vis a vis other groups [Fig. 5(D)]. However, because of the small percentage of the population which falls in this range, it does not achieve the level of significance required. From this population ($\geq$85 μm/s), the differences in the mean percentage of sperm responding to media, from those responding to an increasing gradient, were derived. This gave us the percentage of chemotactic population to be approximately 8.5% which is very close to the range of 2%–12% reported for humans[19] and 10% for mice.[56]

D. Chemotaxis versus chemokinesis

Our results depict that rat sperm demonstrated increased speed and directionality towards increasing ACh concentration as compared to their response in the presence of media devoid of ACh and uniform ACh concentration. Eisenbach's group[10] discerned chemotaxis from chemokinesis on the basis of sperm accumulation in the capillaries when exposed to a decreasing concentration gradient, or uniform concentrations of chemoattractant or media alone. Going by that definition, the response observed for rat sperm to ACh was chemotaxis rather than chemokinesis. Firstly, because the fraction of sperm moving in the direction of increasing ACh concentration was significantly higher than that in the decreasing ACh concentration. In the case of chemokinesis, it has been reported that sperm accumulation in a uniform chemoattractant concentration is higher than that in media devoid of the chemoattractant.[10] However, we observed no difference in the fraction of sperm entering the transverse channels when exposed to a uniform ACh concentration and media control. Hence, we can infer that our microfluidic model could discern sperm chemotaxis from chemokinesis.

E. Sperm response to oviductal fluid

From previous reports in mice, we have seen that crude extract from the egg microenvironment[56] and oviductal fluid from superovulated females[17] proved to have the potential for inducing sperm to move greater distances towards the chemoattractant gradient. We thus assessed sperm response to a biological pool of chemoattractants by using oviductal fluid from the estrus phase rat. In this case, as well, the fraction of spermatozoa responding to the increasing gradient concentration of oviductal fluid was significantly higher compared to the fraction responding to the decreasing concentration gradient, media or uniform concentration of oviductal fluid [Fig. 6(A)]. The fraction of sperm entering the transverse channels from left in media as well as in a uniform concentration of oviductal fluid were below the 0.5 mark. This confirms that sperm exhibit chemotaxis to oviductal fluid concentration gradients.

Further, sperm responded with significantly higher velocities while moving towards an increasing concentration gradient of oviductal fluid compared to their velocities observed in a decreasing gradient, as well as to those in media and a uniform concentration of oviductal fluid [Fig. 6(B)]. As the sperm VSL were found to be similar in either direction when exposed to media as well as with a uniform oviductal fluid concentration, the VSL values for sperm moving in both the directions were combined for the two groups (media and uniform oviductal fluid concentration). On exposure to a single concentration of oviductal fluid, sperm velocities were similar to those observed in media and descending gradient condition suggesting that at the concentration used, the sperm did not demonstrate chemokinetic movement towards the oviductal fluid. Chemotaxis was confirmed with significantly increased velocity for sperm observed in the presence of an uphill gradient of oviductal fluid constituents as compared to media alone, decreasing the gradient and uniform concentration of the oviductal fluid [Fig. 6(B)]. Similar findings were observed with oviductal fluid in mice, with a concentration gradient of 0.1 μg/μl.[17] mRNA expression of Natriuretic Peptide type C, a chemoattractant, present in the oviductal ampulla of mice, has been reported to bring about chemotaxis at nM concentration in an ascending NPPC gradient.[24]

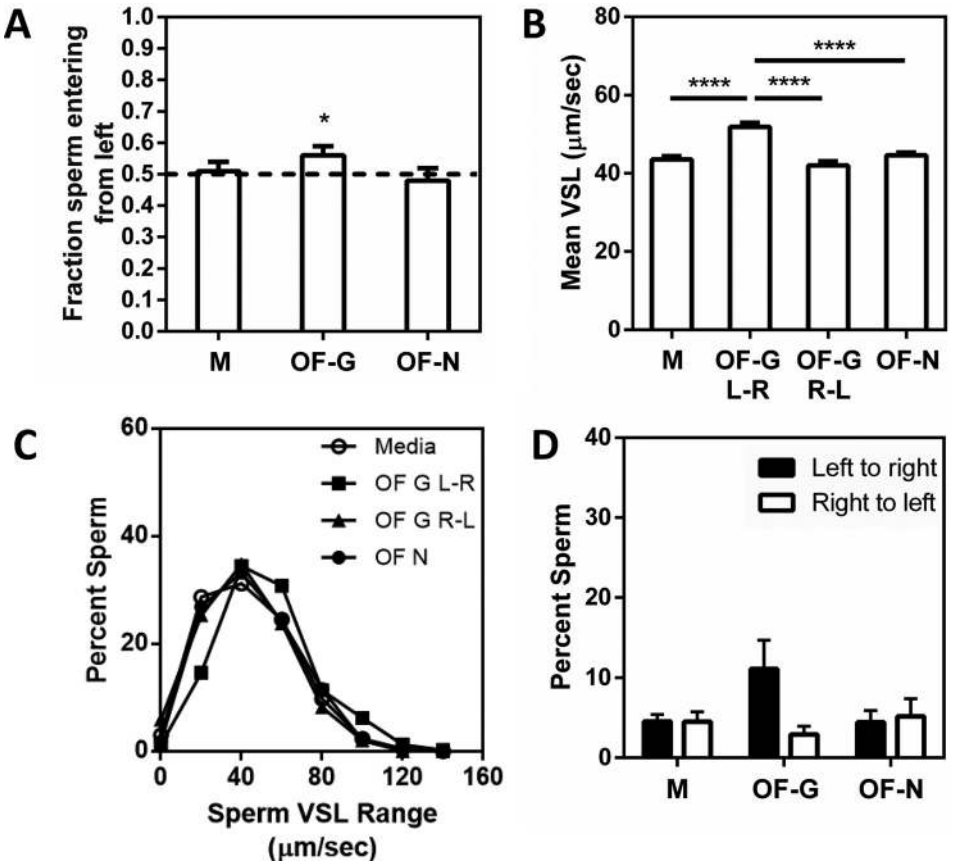

FIG. 6. Sperm response to Oviductal Fluid (OF). Directionality of sperm in the transverse channels in the presence of media, uniform OF concentration or OF gradient (A), sperm VSL in response to the aforementioned conditions (B), distribution profile of sperm VSL (C), and percentage of sperm with VSL $\geq 85\,\mu$m/s under each condition (D). OF-G: gradient of OF; OF-N: uniform concentration of OF; and M: media control. The assay was performed using a single oviductal fluid protein concentration of (∼0.38 g/l) in DMEM. The results are cumulative from 6 experiments in total as detailed in Sec. II. Each column represents mean ± SEM for individual conditions tested. Sperm exhibit a tendency to travel towards higher OF concentration with increased velocities when compared to media and non-gradient conditions. In the case of Fig. "6(B)," as there was no difference in the VSLs for sperm moving in either direction, the VSL values for both the directions were combined in the case of 'M' and 'OF-N' groups, ∼7% of the sperm population demonstrated chemotactic response to OF. "*" $p < 0.05$; "****" $p < 0.00005$.

Plotting the frequency distribution curves for the oviductal fluid demonstrated that the sperm population exposed to an increasing gradient of oviductal fluid had relatively higher percentages of sperm in the 40–80 and 80–120 μm/s VSL range and a lower percentage in the VSL range of 0–40 μm/s as compared to other conditions [Fig. 6(C)]. The chemotactic sperm population was corroborated by the observation of a higher percentage of sperm traveling with velocities above 85 μm/s in the presence of a gradient of oviductal fluid, as compared to the other groups [Fig. 6(D)]. The percentage of chemotactic sperm population to oviductal fluid was calculated as ∼6.6%.

In summary, we have developed a microfluidic chip that could capture sperm chemotaxis. The sperm could be tracked from either side of the transverse channels, which allowed us to study sperm directionality and velocity, in increasing as well as decreasing chemoattractant gradients and in the controls. With the incubation of sperm in a uniform chemoattractant concentration, we were able to distinguish sperm chemotaxis from chemokinesis. The phenomenon of chemotaxis was demonstrated using a known chemoattractant ACh, as well as using a biologically relevant fluid—the oviductal fluid. Thus, our assay could differentiate sperm chemotaxis from other means of sperm accumulation like chemokinesis and trapping and could be categorized as a fusion between directionality and ascending, as well as descending chemoattractant gradient assay.[2]

IV. CONCLUSIONS

We describe here the design and development of a microchip that creates a stable and linear chemoattractant gradient and can discern chemotaxis from chemokinesis. The microfabricated channels facilitated proper fluid flow in the main channels that helped in the maintenance of the gradient in the transverse channels. The mixing zone and the contact zone along with the secondary outlet played a major role in stabilizing flow fluctuations in the presence of cells. Using this device, we demonstrated that ∼6.6% of rat sperm population was chemotactic to oviductal fluid and around 8.5% to ACh, which is in line with that reported by others.[14–17,19] This device can be used to test sperm chemotaxis in response to different biological fluids, as well as to test putative chemoattractants for their chemotactic activity. With minor modifications, the device can be easily used for testing chemotaxis in other cells as well.

ACKNOWLEDGMENTS

The authors thank the nanofabrication facility at the Centre for Excellence in Nanoelectronics (CEN), IIT Bombay, India, and the Experimental animal facility, ICMR-NIRRH, Mumbai, India. We acknowledge the Laser Scanning Confocal Microscope facility at the Department of Biosciences and Bioengineering, IIT Bombay, India. We also thank Dr. Shahaina Begum, NIRRH for her advice on statistical analysis of data and Mr. Mahadev Merchande, NIRRH for help with animal handling. We acknowledge funding support from the Department of Biotechnology (DBT) [(P.P. and S.J.; Grant # BT/PR13442/MED/32/440/2015), DBT (S.J.; Grant # BT/PR7741/MED/32/275/2013)], the Council of Scientific and Industrial Research India [S.J.; Grant # 22/(06840)/15/EMR-II], the Healthcare Research Consortium at IIT Bombay (S.J. and P.P.; Grant # 12IRSGHC005), and the Indian Council of Medical Research (P.P.; RA/602/01-2018). We also acknowledge Dr. Smita Mahale, Director, ICMR - NIRRH, Mumbai, India, for her support and co-ordinating the project.

[1]S. S. Suarez and A. A. Pacey, Hum. Reprod. Update **12**, 23 (2006).
[2]M. Eisenbach and L. C. Giojalas, Nat. Rev. Mol. Cell Biol. **7**, 276 (2006).
[3]M. Eisenbach, S. Cerezales, and S. Boryshpolets, Asian J. Androl. **17**, 628 (2015).
[4]S. S. Suarez, Cell Tissue Res. **363**, 185 (2016).
[5]K. Miki and D. E. Clapham, Curr. Biol. **23**, 443 (2013).
[6]C. Tung, F. Ardon, A. G. Fiore, S. S. Suarez, and M. Wu, Lab Chip **14**, 1348 (2014).
[7]T. M. El-Sherry, M. Elsayed, H. K. Abdelhafez, and M. Abdelgawad, in *Proceedings of the 7th Cairo International Biomedical Engineering Conference CIBEC 2014* (2015), Vol. 6, p. 181.
[8]A. Bahat, I. Tur-Kaspa, A. Gakamsky, L. C. Giojalas, H. Breitbart, and M. Eisenbach, Nat. Med. **9**, 149 (2003).
[9]A. Bahat and M. Eisenbach, Mol. Cell. Endocrinol. **252**, 115 (2006).
[10]D. Ralt, M. Manor, A. Cohen-Dayag, I. Tur-Kaspa, I. Ben-Shlomo, A. Makler, I. Yuli, J. Dor, S. Blumberg, S. Mashiach, and M. Eisenbach, Biol. Reprod. **50**, 774 (1994).
[11]Z. Zhang, J. Liu, J. Meriano, C. Ru, S. Xie, J. Luo, and Y. Sun, Sci. Rep. **6**, 23553 (2016).
[12]A. Bahat, S. R. Caplan, and M. Eisenbach, PLoS One **7**, e41915 (2012).
[13]A. Cohen-Dayag, I. Tur-Kaspa, J. Dor, S. Mashiach, and M. Eisenbach, Proc. Natl. Acad. Sci. U.S.A. **92**, 11039 (1995).
[14]L. Xie, R. Ma, C. Han, K. Su, Q. Zhang, T. Qiu, L. Wang, G. Huang, J. Qiao, J. Wang, and J. Cheng, Clin. Chem. **56**, 1270 (2010).
[15]M. E. Teves, F. Barbano, H. A. Guidobaldi, R. Sanchez, W. Miska, and L. C. Giojalas, Fertil. Steril. **86**, 745 (2006).
[16]S. Koyama, D. Amarie, H. A. Soini, M. V. Novotny, and S. C. Jacobson, Anal. Chem. **78**, 3354 (2006).
[17]R. G. Oliveira, L. Tomasi, R. A. Rovasio, and L. C. Giojalas, J. Reprod. Fertil. **115**, 23 (1999).
[18]L. A. Burnett, D. M. Anderson, A. Rawls, A. L. Bieber, and D. E. Chandler, Dev. Biol. **360**, 318 (2011).
[19]A. Cohen-Dayag, D. Ralt, I. Tur-Kaspa, M. Manor, A. Makler, J. Dor, S. Mashiach, and M. Eisenbach, Biol. Reprod. **50**, 786 (1994).
[20]C. Villanueva-Diaz, F. Vadillo-Ortega, A. Kably-Ambe, M. A. Diaz-Perez, and S. K. Krivitzky, Fertil. Steril. **54**, 1180 (1990).
[21]N. Zamir, R. Riven-Kreitman, M. Manor, A. Makler, S. Blumberg, D. Ralt, and M. Eisenbach, Biochem. Biophys. Res. Commun. **197**, 116 (1993).
[22]L. Śliwa, Eur. J. Obstet. Gynecol. Reprod. Biol. **58**, 173 (1995).
[23]C. Villanueva-Diaz, J. Arias-Martinez, L. Bermejo-Martinez, and F. Vadillo-Ortega, Fertil. Steril. **64**, 1183 (1995).
[24]N. Kong, X. Xu, Y. Zhang, Y. Wang, X. Hao, Y. Zhao, J. Qiao, G. Xia, and M. Zhang, Sci. Rep. **7**, 39711 (2017).
[25]P. Caballero-Campo, M. G. Buffone, F. Benencia, J. R. Conejo-García, P. F. Rinaudo, and G. L. Gerton, J. Cell. Physiol. **229**, 68 (2014).
[26]T. Isobe, H. Minoura, K. Tanaka, T. Shibahara, N. Hayashi, and N. Toyoda, Hum. Reprod. **17**, 1441 (2002).
[27]Y. Wang, R. Storeng, P. O. Dale, T. Åbyholm, and T. Tanbo, Gynecol. Endocrinol. **15**, 286 (2001).
[28]B. S. Jaiswal, I. Tur-Kaspa, J. Dor, S. Mashiach, and M. Eisenbach, Biol. Reprod. **60**, 1314 (1999).
[29]H. A. Guidobaldi, M. E. Teves, D. R. Unates, A. Anastasia, and L. C. Giojalas, PLoS One **3**, e3040 (2008).
[30]R. Oren-Benaroya, R. Orvieto, A. Gakamsky, M. Pinchasov, and M. Eisenbach, Hum. Reprod. **23**, 2339 (2008).

[31]L. Sliwa, Arch. Androl. **35**, 105 (1995).
[32]M. Steffl, M. Schweiger, I. Wessler, L. Kunz, A. Mayerhofer, and W. M. Amselgruber, Anat. Embryol. **211**, 685 (2006).
[33]J. Urra, J. Blohberger, M. Tiszavari, A. Mayerhofer, and H. E. Lara, Sci. Rep. **6**, 1 (2016).
[34]J. Wu, X. Wu, and F. Lin, Lab Chip **13**, 2484 (2013).
[35]Y.-J. Ko, J.-H. Maeng, B.-C. Lee, S. Lee, S. Y. Hwang, and Y. Ahn, Anal. Sci. **28**, 27 (2012).
[36]H. Chang, B. J. Kim, Y. S. Kim, S. S. Suarez, and M. Wu, PLoS One **8**, e60587 (2013).
[37]Y. Zhang, R. R. Xiao, T. Yin, W. Zou, Y. Tang, J. Ding, and J. Yang, PLoS One **10**, e0142555 (2015).
[38]M. V. Inamdar, T. Kim, Y. Chung, A. M. Was, X. Xiang, C. Wang, S. Takayama, C. M. Lastoskie, F. I. M. Thomas, and A. M. Sastry, J. Exp. Biol. **210**, 3805 (2007).
[39]M. Eisenbach, Rev. Reprod. **4**, 56 (1999).
[40]D. K. and S. Jadhav, Chem. Eng. Process. - Process Intensif. **124**, 155 (2018).
[41]Y. H. Hussain, J. S. Guasto, R. K. Zimmer, R. Stocker, and J. A. Riffell, J. Exp. Biol. **219**, 1458 (2016).
[42]M. Eisenbach and I. Tur-Kaspa, Fertil. Steril. **62**, 233 (1994).
[43]D. Irimia, G. Charras, N. Agrawal, T. Mitchison, and M. Toner, Lab Chip **7**, 1783 (2007).
[44]J. Qiao, H. Zhao, Y. Zhang, H. Peng, Q. Chen, H. Zhang, X. Zheng, Y. Jin, H. Ni, E. Duan, and Y. Guo, Theriogenology **88**, 98 (2017).
[45]S. K. W. Dertinger, D. T. Chiu, N. L. Jeon, and G. M. Whitesides, Anal. Chem. **73**, 1240 (2001).
[46]G. M. Whitesides, E. Ostuni, S. Takayama, X. Jiang, and D. E. Ingber, Annu. Rev. Biomed. Eng. **3**, 335 (2001).
[47]N. Li Jeon, H. Baskaran, S. K. W. Dertinger, G. M. Whitesides, L. Van De Water, and M. Toner, Nat. Biotechnol. **20**, 826 (2002).
[48]M. M. Bradford, Anal. Biochem. **72**, 248 (1976).
[49]J. Xia and D. Ren, Reprod. Biol. Endocrinol. **7**, 119 (2009).
[50]C. H. Yeung, G. Oberlander, and T. G. Cooper, J. Reprod. Fertil. **96**, 427 (1992).
[51]J. Seed, R. E. Chapin, E. D. Clegg, L. A. Dostal, R. H. Foote, M. E. Hurtt, G. R. Klinefelter, S. L. Makris, S. D. Perreault, S. Schrader, D. Seyler, R. Sprando, K. A. Treinen, D. N. R. Veeramachaneni, and L. D. Wise, Reprod. Toxicol. **10**, 237 (1996).
[52]C. A. Schneider, W. S. Rasband, and K. W. Eliceiri, Nat. Methods **9**, 671 (2012).
[53]F. Sun, L. C. Giojalas, R. A. Rovasio, I. Tur-Kaspa, R. Sanchez, and M. Eisenbach, Dev. Biol. **255**, 423 (2003).
[54]P. Kumar and S. Meizel, J. Biol. Chem. **280**, 25928 (2005).
[55]C. Bray, J.-H. Son, P. Kumar, and S. Meizel, Biol. Reprod. **73**, 807 (2005).
[56]L. C. Giojalas and R. A. Rovasio, Int. J. Androl. **21**, 201 (1998).